

# Variable guiding strategies in multi-exits evacuation: Pursuing balanced pedestrian densities

Huan Ren<sup>a</sup>, Yuyue Yan<sup>b,\*</sup>, Fengqiang Gao<sup>a</sup>

<sup>a</sup>*School of Information Science Technology, Xiamen University Tan Kah Kee College, Fujian 363105, China*

<sup>b</sup>*Department of Systems and Control Engineering, Tokyo Institute of Technology, Tokyo 152-8552, Japan*

## Abstract

Evacuation assistants and their guiding strategies play an important role in the multi-exits pedestrian evacuation. To investigate the effect of guiding strategies on evacuation efficiency, we propose a force-driven cellular automaton model with adjustable guiding attractions imposed by the evacuation assistants located in the exits. In this model, each of the evacuation assistants tries to attract the pedestrians in the evacuation space towards its own exit by sending a quantifiable guiding signal, which may be adjusted according to the values of pedestrian density near the exit. The effects of guiding strategies pursuing balanced pedestrian densities are studied. It is observed that the unbalanced pedestrian distribution is mainly yielded by a snowballing effect generated from the mutual attractions among the pedestrians, and can be suppressed by controlling the pedestrian densities around the exits. We also reveal an interesting fact that given a moderate target density value, the density control for the partial regions (near the exits) could yield a global effect for balancing the pedestrians in the rest of the regions and hence improve the evacuation efficiency. Our findings may contribute to give new insight into designing effective guiding strategies in the realistic evacuation process.

**Keywords:** Force-driven cellular automaton model; pedestrian flow; guided crowd; evacuation efficiency; evacuation simulation.

## 1. Introduction

The efficiency estimation for pedestrian evacuation is a key aspect of safety performance evaluation when the earthquake, fire, terrorist attacks, and other emergencies occur in public places. During the evacuation process, pedestrians may possess some irrational behaviors such as anxiety, panic and blindly following, to name but a few, which may affect the evacuation efficiency and hence cause some casualties and property losses [1–4]. To avoid such cases, it is significantly important to understand the pedestrian behaviors in the evacuation process [5–7]. In the literature, the existing pedestrian dynamics are mainly categorized to the continuous-time and discrete-time models [8–18]. As the typical discrete-time dynamics, the cellular automaton models provide a structure for reflecting the pedestrians' microscopic characteristics with some simple update laws (evolution rules), which may be combined with the notion of social force [19], floor field [9, 20], etc. For instant, Huang et al. established a cellular automaton model to describe the movement of heterogeneous pedestrians in terms of cooperative behavior and examined how the dynamics of dependency relationship among the pedestrians affect the evacuation efficiency [21]. Pereira et al. extend the cellular automaton model to allow pedestrians to change direction for accessing an alternate exit route [22]. Miyagawa and Ichinose proposed a multi-grid cellular automaton model with turning behavior [23].

\*Corresponding author.

Email address: [yan.y.ac@m.titech.ac.jp](mailto:yan.y.ac@m.titech.ac.jp) (Yuyue Yan)

During the emergency evacuation, some evacuation assistants are usually adopted to help evacuees escape as soon as possible. The related works in terms of guided behaviors in evacuation can be found in [24–30]. In those works, most of the scholars only discussed the single-exit evacuation scenario based on a social force model. For example, Yang et al. [24] first claimed the necessity of guides in pedestrian emergency evacuation. Ma et al. [25, 26] considered dynamic leaders inside a room who attract the crowds and move together with them towards a unique exit with different pedestrian densities. It was found in [25] that a large evacuees crowd can be efficiently guided by those dynamic evacuation assistants if the neighbor density is moderate. However, the possibility and effects of controlling the pedestrian densities are not considered yet.

Different from the existing works, in this paper, we consider the situation where multiple evacuation assistants locate in their corresponding exits and may try to adjust their guiding signals to attract the crowds under density control. It is well known that the balanced pedestrians evacuation could improve the evacuation efficiency [31]. Hence, we mainly focus on pursuing balanced pedestrian densities in a cellular automaton-based evacuation model with multiple exits, and discuss the inherent relation between the evacuation efficiency and the balanced pedestrian densities. Specifically, we suppose that each of the evacuation assistants measures the pedestrian density around its own exit and changes the guiding strategies (i.e., the strength of the guiding signal) according to the measured data.

The contributions of this paper are summarized as follows. 1) We propose a novel force driven cellular automaton model with multiple exits and variable guiding strategies, where the strength of the guiding signal for each of the exits (evacuation assistants) is adjustable according the evacuation situation. 2) The reason why unbalanced pedestrian distribution yielded in the evacuation process is interpreted. 3) Two different density control laws for obtaining the on-off and quantifiable guiding signals are characterized for suppressing the unbalanced pedestrian distribution. The relation between the target density and the evacuation efficiency for each of the proposed control laws is discussed and the optimal target density is numerically found for a square evacuation space.

The rest of this paper is organized as follows: A novel force driven cellular automaton model with multiple exits and variable guiding strategies as well as the two designed density control laws are proposed in Section 2. In Section 3, we first interpret the fact that the guiding behaviors without density control may waste the capacity of the exits, and then we apply the density control laws designed in Section 2 to the evacuation model to observe the effects of the control behaviors for the evacuation process. The comparisons of the evacuation efficiencies with and without density control are also given in Section 3. Finally, we conclude our paper in Section 4.

*Notation:* In this paper, we write  $\mathbb{R}_+$  for the set of positive real numbers,  $\mathbb{N}_+$  for the set of positive integers and  $\emptyset$  for the empty set.

## 2. Model

In this section, we propose our pedestrian evacuation model based on force-driven cellular automaton [19] with *time-varying* guiding signals. In this model, the state space (i.e., evacuation space) is divided to  $N \times N$  number of cells where each of the cells may be occupied by a single pedestrian. At each time instant (or, equivalently, time step), the pedestrians may have multiple desired moving directions and need to compete with the others if the desired cell is targeted by more than one pedestrians. For each of the pedestrians, we assume that there are eight possible moving directions whose corresponding cells neighbor to the current location (cell). Defining a social (resultant) force consisting of a guiding force from an evacuation assistant, interaction forces among pedestrians and an attractive force from a visible exit, the moving direction candidates for each of the pedestrians can be properly given according to the directions of the decomposed forces at  $x$ ,  $y$ ,  $s$  and  $f$ -axis illustrated in Fig. 1 below, where the preferences of those moving direction candidates solely depend on the magnitudes of the decomposed forces. In the following statements, we first define the component forces for the pedestrians to describe their self-organization behaviors and then present the evolution rules for the proposed model.

### 2.1. Component Forces

Denoting  $\mathbb{RM}(k)$  as the set of remaining pedestrians in the state space at the time instant  $k = 0, 1, 2, \dots$ , we define the component social forces for the pedestrian  $n \in \mathbb{RM}(k)$  in the following statements.

#### 2.1.1. Guiding Force

In reality, the pedestrians may receive guiding signals (i.e., instructions) from the evacuation assistant(s), e.g., sound, action and warning lights, and hence the moving directions and evacuation efficiency are significantly influenced. In this paper, we assume that each of the exits possesses an independent evacuation assistant who attract the

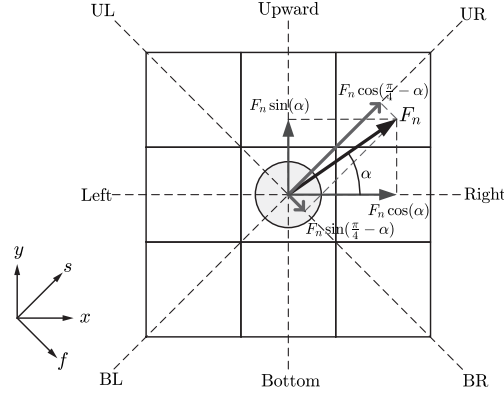


Figure 1. Decomposed forces in  $x$ ,  $y$ ,  $s$  and  $f$  axis. The ranking on the magnitudes of decomposed forces is given by upper right, right, upward and bottom right and hence this pedestrian is assumed to prefer those four directions as the next moving directions. If the preferred moving direction is in a conflict with the other pedestrian, then a competition is considered to determine the winner who occupy the competed cell in the next time instant (time step). If the pedestrian lost in all of the competitions for the four preferred moving directions, then he remains in the original cell in the next time instant.

pedestrians  $n \in \mathbb{RM}(k)$  towards its own exit. Let  $\mathcal{N} \triangleq \{1, \dots, N_e\}$  denote the set of exits (or, evacuation assistant) where  $N_e$  denotes the number of exits. For each of the pedestrians  $n \in \mathbb{RM}(k)$ , the guiding force is defined by

$$F_{\text{guide}}^n = u_{I_n} D \vec{r}_{n,I_n}, \quad (1)$$

where  $I_n \in \mathcal{N}$  denotes the index of the evacuation assistant believed by the pedestrian  $n$ ,  $\vec{r}_{n,I_n}$  denotes a unit vector from the pedestrian  $n$  to the exit  $I_n$ ,  $D \in \mathbb{R}_+$  denotes the maximal guiding intensity, and  $u_{I_n} \in [0, 1] \subset \mathbb{R}$ ,  $I_n \in \mathcal{N}$ , denote coefficients designed (or controlled) by the evacuation assistants  $I_n \in \mathcal{N}$ . If  $u_i$  is taken as a zero (resp., nonzero) value, then it is understood that the evacuation assistant  $i \in \mathcal{N}$  stops attracting (resp., tries to attract) the pedestrians  $n \in \mathbb{RM}(k)$ . Inspired by the notion of *signal to interference ratio*, we consider

$$I_n \triangleq \arg \max_{i \in \mathcal{N}} \left( \frac{u_i}{1 + \sum_{j \in \mathcal{N} \setminus \{i\}} (r_{n,i}^2 / r_{n,j}^2)} \right), \quad (2)$$

with  $r_{n,i} \in \mathbb{R}_+$  denoting the distance (step length) from the pedestrian  $n$  to the exit  $i$ ,  $i \in \mathcal{N}$ . Note that the expression in the right-hand side of Eq. (2) represents the reliability of the guiding signal from the evacuation assistant  $i \in \mathcal{N}$ . Specifically, if  $u_i = 1$ ,  $i \in \mathcal{N}$ , then the pedestrian  $n$  is attracted by the nearest evacuation assistant. However, if the nearest evacuation assistant  $i \in \mathcal{N}$  turns off its guiding signal, i.e.,  $u_i = 0$ , then the pedestrian  $n$  is attracted by the other evacuation assistants. Hence, we note that the coefficients  $u_i$ ,  $i \in \mathcal{N}$ , may be time-varying according to the strategies of the evacuation assistants (see the controlled coefficients  $u_i$ ,  $i \in \mathcal{N}$ , in Section 2.4 below).

### 2.1.2. Mutual forces among pedestrians

The existence of mutual forces among the pedestrians is the main reason of herding effect. Let  $\mathbb{VP}_n$  denote the set of visible pedestrians for the pedestrian  $n \in \mathbb{RM}(k)$ , i.e., the distance  $r_{nm} \in \mathbb{N}_+$  from the pedestrian  $n$  to  $m$  is smaller than a constant integer  $w \in \mathbb{N}_+$  for all  $m \in \mathbb{VP}_n$ . According to the distance  $r_{nm}$ , we define the mutual force

$$F_{\text{mutual}}^{n,m} = \begin{cases} -\eta_1 \vec{r}_{n,m}, & \text{if } r_{n,m} = 1 \\ \eta_2 / r_{n,m}^2 \vec{r}_{n,m}, & \text{if } 1 < r_{n,m} \leq w \end{cases}, \quad m \in \mathbb{VP}_n, \quad (3)$$

where  $\eta_1 \in \mathbb{R}_+$  denotes a coefficient for repulsion,  $\eta_2 \in \mathbb{R}_+$  denotes a coefficient for attraction,  $\vec{r}_{n,m}$  denotes a unit vector from the pedestrian  $n$  to the visible pedestrian  $m$ , and  $w$  denotes the length of the filed of view.

### 2.1.3. Attractive force to a visible exit

If one of the exits appears in the visible region, the pedestrian  $n \in \mathbb{RM}(k)$  is supposed to possess an attractive force to the visible exit, which is defined by

$$F_{\text{exit}}^{n,i} = E \vec{r}_{n,i}, \quad i \in \mathbb{VE}_n \triangleq \{i \in \mathcal{N} : r_{n,i} \leq w\}, \quad (4)$$

where  $E \in \mathbb{R}_+$  denotes a constant value,  $r_{n,i}$  and  $\vec{r}_{n,i}$  denote the distance and the unit vector from the pedestrian  $n$  to the exit  $i \in \mathcal{N}$ , respectively.

## 2.2. Resultant force and preference moving direction

Consequently, for a pedestrian  $n \in \mathbb{RM}(k)$ , the resultant social force is defined by

$$F_n = w_1 F_{\text{guide}}^n + w_2 \sum_{i \in \mathbb{VE}} F_{\text{exit}}^{n,i} + w_3 \sum_{m \in \mathbb{VP}} F_{\text{mutual}}^{n,m}, \quad (5)$$

where  $w_1, w_2$  and  $w_3 \in \mathbb{R}_+$  denote the positive weighting factors depending on the evacuation scenario. For instant, the influence of guiding signal and visible exit may be *weakened* (i.e.,  $w_1 < w_3$  and  $w_2 < w_3$  hold) when the pedestrians are trapped by panic as the space is full of the smoke of fire. We assume that the preferences of moving direction candidates for the pedestrian  $n \in \mathbb{RM}(k)$  are determined by sorting the magnitude of the decomposed forces of  $F_n$  at  $x, y, s$  and  $f$ -axis (see Fig. 1). For example, denoting the cell address at the upward, right, upper right and bottom right directions by  $Q_{\text{Upward}}^n, Q_{\text{Right}}^n, Q_{\text{UR}}^n$ , and  $Q_{\text{BR}}^n$ , the ordered preference target cells in Fig. 1 are given by  $[Q_{\text{UR}}^n, Q_{\text{Right}}^n, Q_{\text{Upward}}^n, Q_{\text{BR}}^n]$ . However, if one of the preferred target cells is already occupied, then the corresponding decomposed force is understood as zero and hence the sequence of ordered preference target cells may be altered. For the following statements, we define  $P_n = [P_n^1, P_n^2, P_n^3, P_n^4]$  as the sequence of ordered preference target cells where  $P_n^i$  denotes the address of the  $i$ -th preferred target. Here, it is important to note that even though the preference target cells are deterministic, there may still exist some *stochastic* processes among deciding addresses of pedestrians at the next time instant, which are described as *random competitions* shown in Section 2.3 ii) below.

## 2.3. Evolution rules

Given an initial set  $\mathbb{RM}(k)$  with  $k = 0$ , the evolution rules are summarized as follows.

i) Each of the pedestrians  $n \in \mathbb{RM}(k)$  remaining in the state space calculates his own resultant social force according to Eqs. (1)–(5), and determines his ordered preference target cells (unoccupied) as moving direction candidates according to the magnitude of the decomposed forces.

ii) Target competition. Recalling that multiple pedestrians may have the same preferred target cells, which is so called ‘collision effect’ in [32] and [33], we consider target competitions among the pedestrians to solve the collisions. In particular, we assume that each pedestrian  $n$  conflicting with the others possesses at most 4 rounds of chances to compete for the preferred target cell according to the sequence  $P_n$ . If the pedestrian  $n$  wins in the competition at the round  $i = 1, 2, 3, 4$ , then his  $i$ -th preferred target cell (i.e.,  $P_n^i$ ) is assigned to him as the address at next time instant and the others compete for the next un-assigned preferred target cell. If the pedestrian loses in all the competitions, then he stays in his current location at next time instant because of the *unsolvable collisions*. Here, we assume the winner is *randomly* selected in the competitions.

iii) Update the addresses for all the pedestrians and delete the pedestrians who reach one of the exits. Let  $k = k + 1$  and update the set  $\mathbb{RM}(k)$ .

iv) If all of pedestrians have left the state space, i.e.,  $\mathbb{RM} = \emptyset$ , the program ends. Otherwise, go to i) to continue.

**Remark 1** Note that depending on the parameters defined in Section 2.1 and Eq. (5), our proposed model can reflect various evacuation situations such as emergent evacuations in face of potential risk, and the ones considering panic evacuees, illegible exits and time-varying guiding signals. For example, supposing that  $w_2$  in Eq. (5) is very small but  $\eta_2$  in Eq. (3) is very large, the proposed model can reflect the scenario where evacuees are exposed to critical situation such as fires. In such a case, the pedestrians may hardly find the exits in their visions, be trapped by panic, and never leave the evacuation space in the simulation.

## 2.4. Strategy on coefficients $u_i, i \in \mathcal{N}$

In the following sections, we investigate the strategies to change the coefficients  $u_i, i \in \mathcal{N}$ , for adjusting the guiding strength of the evacuation assistants. Specifically, we consider pedestrian density control in the evacuation and characterize its influence to the evacuation efficiency. Let  $\rho_i$  denote the pedestrian density near the exit  $i \in \mathcal{N}$ , which is sampled by the corresponding evacuation assistant. We utilize two schemes to update the values of  $u_i, i \in \mathcal{N}$ .

1) Scheme 1 (Bang-bang control): Let  $\rho_{\text{aim}}$  be a target density. The values of  $u_i, i \in \mathcal{N}$ , are determined by

$$u_i(k) = \begin{cases} 1, & \rho_i(k-1) \leq \rho_{\text{aim}}, \\ 0, & \rho_i(k-1) > \rho_{\text{aim}}, \end{cases} \quad i \in \mathcal{N}, \quad k = 1, 2, 3, \dots, \quad (6)$$

where the guiding signal is off (resp., on) when the current density is larger (resp., smaller) than the target density.

2) Scheme 2 (PI control): Suppose  $u_i, i \in \mathcal{N}$ , are quantifiable. Let  $\rho_{\text{aim}}$  be a target density and let  $e(k) = \rho_i(k) - \rho_{\text{aim}}$ . The values of  $u_i, i \in \mathcal{N}$ , are determined by the following update laws

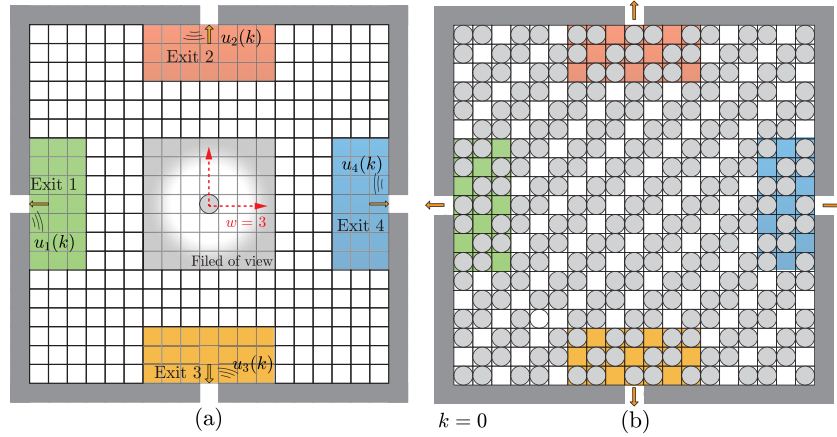


Figure 2. Evacuation space (i.e., state space) and initial distribution in simulations. (a): Simulation environment with  $N = 19$  and  $\mathcal{N} = \{1, 2, 3, 4\}$ , where the colored areas near exits denote the regions used for observing (or, calculating) pedestrian densities, (b): initial distribution of pedestrians ( $\mathbb{RM}(0)$  includes 241 elements) where circles denote the pedestrians.

$$u_i(k) = u_i(k-1) + K_p e(k) + K_i \sum_{j=0}^k e(j), \quad i \in \mathcal{N}, \quad k = 1, 2, 3, \dots, \quad (7)$$

where  $K_p$  and  $K_i$  are some positive constants. Under the above update law, the guiding strength is reduced (resp., increased) when the current density is larger (resp., smaller) than the target density.

### 3. Simulation and Results

In this section, we present the simulation results of the proposed model under the different strategies in terms of  $u_i(k)$ ,  $i \in \mathcal{N}$ . We consider a square room with  $N_e = 4$  exits as the evacuation environment, i.e.,  $\mathcal{N} = \{1, 2, 3, 4\}$ . We divide the evacuation environment to  $19 \times 19$  cells and establish the state space as illustrated in Fig. 2(a), where the length of the filed of view is set to 3 (i.e.,  $w = 3$ ) and the 4 regions for observing pedestrian densities are given. The initial amount of pedestrians is set to 241. Pedestrians at the time instant  $k = 0$  are distributed as Fig. 2(b). Since each of the 4 regions near the exits only possesses 21 cells, the pedestrian density near the exit  $i \in \mathcal{N}$  is measured as  $\rho_i(k) = \text{num}_i(k)/21$ , where  $\text{num}_i$  denotes the number of pedestrians located in the region  $i$ . Hence it can be seen from Fig. 2(b) that the initial pedestrian densities in all of the 4 regions are the same as each other and given by  $\rho_i(0) = 0.667$ ,  $i \in \mathcal{N}$ . The maximal guiding intensity is set to 30 (i.e.,  $D = 30$  in Eq. (1)), the parameter for attractive force to a visible exit is set to 40 (i.e.,  $E = 40$  in Eq. (4)), and the coefficient for mutual repulsion (resp., attraction) among the pedestrians is set to 0.6 (resp., 1.2), i.e.,  $\eta_1 = 0.6$  and  $\eta_2 = 1.2$  in Eq. (3). The weighting factors in Eq. (5) are set to  $w_1 = w_2 = w_3 = 1$ .

#### 3.1. Compared Parameters

We define the following two notions to compare the evacuation efficiency.

A) Unbalanced degrees in terms of density:  $\alpha_i$ ,  $i \in \mathcal{N}$

Unbalanced factor  $\alpha_i$  represents how much the pedestrian density near the exit  $i \in \mathcal{N}$  is unbalanced comparing to the ones for the other exits, and is given by

$$\alpha_i(k) = \left| \frac{\rho_i(k)}{\sum_{j \in \mathcal{N}} \rho_j(k)} - \frac{c_i}{\sum_{j \in \mathcal{N}} c_j} \right|, \quad i \in \mathcal{N}, \quad k = 1, 2, 3, \dots, \quad (8)$$

where  $\rho_i$  denotes the pedestrian density near the exit  $i$  (see the colored region in Fig. 2(a)),  $i \in \mathcal{N}$ , and  $c_i$  denotes a constant value representing the capacity of exit  $i$ . Since all the exits considered in Fig. 2 have the same size and hence same capacity, we have  $\alpha_i(k) = \left| \frac{\rho_i(k)}{\sum_{j \in \mathcal{N}} \rho_j(k)} - \frac{1}{N_e} \right| \in \left[ 0, \frac{N_e-1}{N_e} \right]$ .

B) Travel time:  $T_{\text{end}}$

Travel time is the number of steps which the last pedestrian used to leave to the exit, i.e.,  $\mathbb{RM}(k) = 0$  at  $k = T_{\text{end}}$ . Note that if the unbalanced degree maintain as a large number, then it is understood that the capacities of some exits are not efficiently utilized. In this case,  $T_{\text{end}}$  is probably larger than the case of balanced pedestrian density.



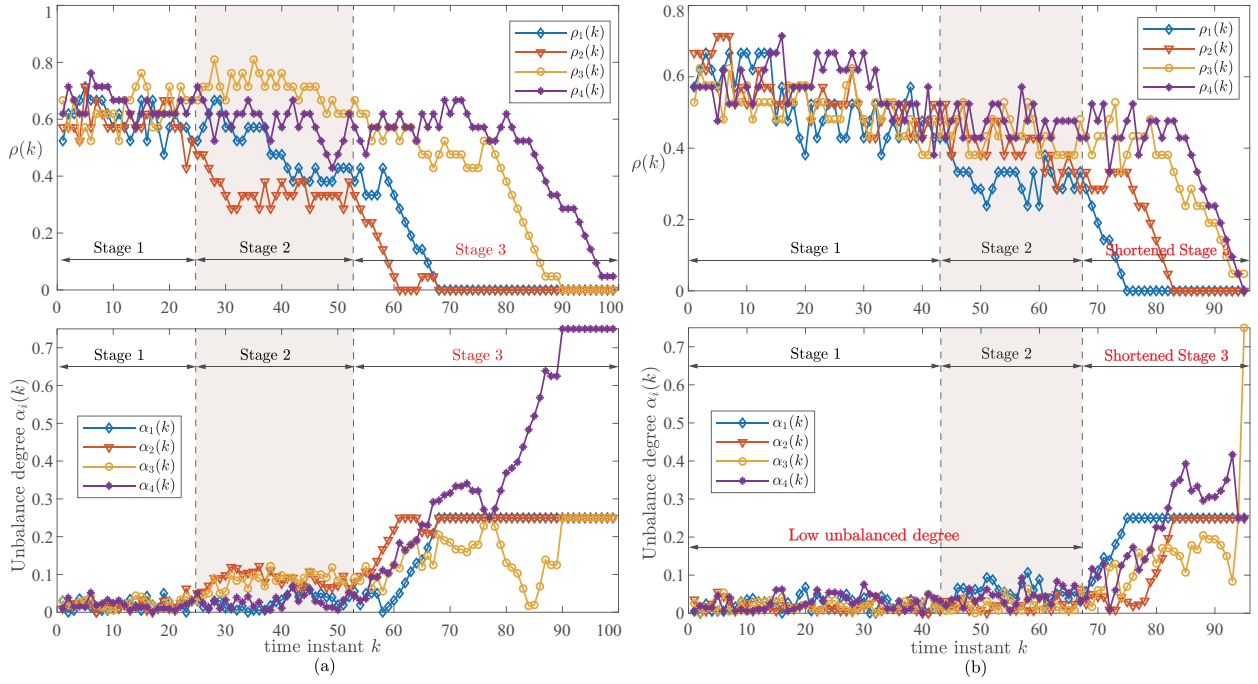


Figure 3. Trajectories of pedestrian densities and unbalanced degrees. (a) Without control ( $u_i(k) = 1, i \in \mathcal{N}, k = 1, 2, \dots, \infty$ ), (b) Under Bang-bang control Eq. (6) with  $\rho_{\text{aim}} = 0.5$ . The evacuation process without control possesses a long period with extremely unbalanced densities near the 4 exits in (a) (which is referred to as stage 3). In (b), unbalanced behaviors are suppressed under density control and the period of stage 3 is shortened.

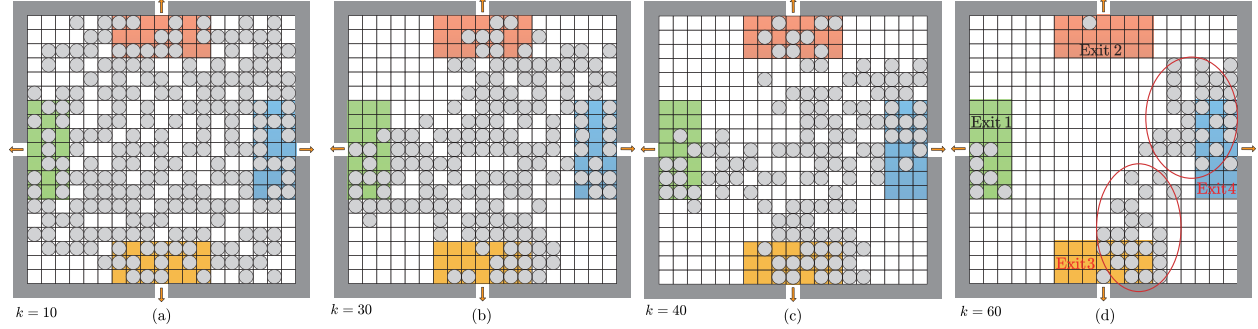


Figure 4. Pedestrian distributions at the typical time instants without control ( $u_i(k) = 1, i \in \mathcal{N}, k = 1, 2, \dots, \infty$ ). (a):  $k = 10$ , (b):  $k = 30$ , (c):  $k = 40$ , (d):  $k = 60$ . The distributions of pedestrians are more and more unbalanced along with the time instants, especially at  $k = 60$ .

### 3.2. Simulation Results Without Density Control

To investigate the effects of density control on evacuation efficiency, we first present the simulation results without the density control, i.e.,  $u_i(k) = 1, i \in \mathcal{N}, k = 1, 2, \dots, \infty$ . In this case, each of the evacuation assistants ignores the real value of pedestrian density near its own exit and tries to attract the pedestrians all the times. Hence, it follows from Eq. (2) that the pedestrians are attracted by the nearest evacuation assistant from their own locations. In the simulation, it is found that the pedestrians used 100 time steps to leave the state space, i.e.,  $T_{\text{end}} = 100$ . The trajectories of the pedestrian densities near the exits 1, 2, 3, 4 and the corresponding unbalanced degrees  $\alpha_i(k), i \in \mathcal{N}, k = 1, 2, \dots, T_{\text{end}}$ , are shown in Fig. 3 (a). It can be seen from the figure that the tendency of pedestrian densities includes 3 obvious different stages. 1) In the beginning (which is henceforth referred to as “stage 1”), the pedestrian densities in different exits are very similar to each other (e.g., see the typical example of pedestrian distribution at time instant  $k = 10$  in Fig. 4(a)); 2) Some slight but visible unbalanced phenomena appear along with the time instants, which we call “stage 2”. The typical examples of pedestrian distribution at stage 2 are illustrated in Figs. 4(b) and 4(c), where the time instants are given by  $k = 30$  and 40, respectively. It can be seen from those figures that more and more pedestrians begin to be attracted to the exits 3 and 4. Those slight unbalanced phenomena are caused by the herding effects

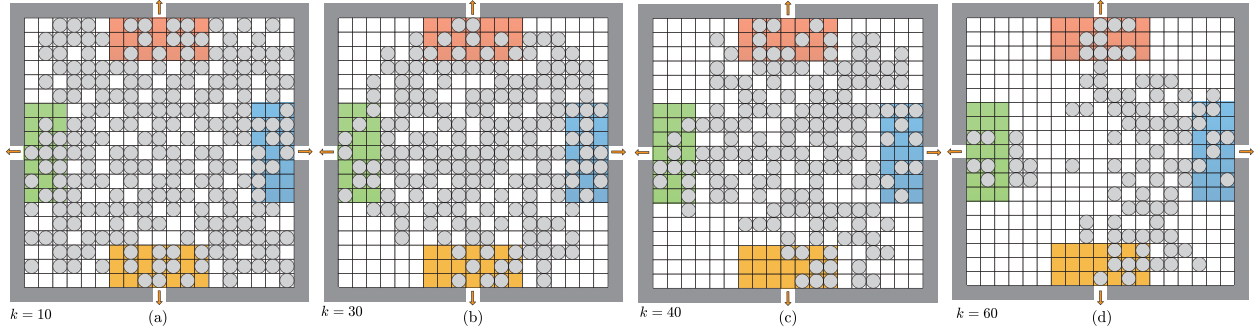


Figure 5. Pedestrian distributions at the typical time instants under Bang-bang control with  $\rho_{\text{aim}} = 0.5$ . (a):  $k = 10$ , (b):  $k = 30$ , (c):  $k = 40$ , (d):  $k = 60$ . Comparing to Fig. 4, the unbalanced behaviors are certainly suppressed, i.e., distributions of pedestrians are more balanced near the four exits. For example, at time instant  $k = 60$ , the crowd is mainly near the exits 2, 3 and 4 instead of only near the exits 3 and 4 in Fig. 4(d).

generated from mutual attractions among the pedestrians. Even if only a few of the pedestrians are closing to one of the exits in an unbalanced way by coincidence, the neighbor pedestrians may be attracted to the same direction and the amount of affected pedestrians may keep growing like a snowballing effect and hence eventually the unbalanced phenomena became extremely visible; 3) Therefore, it is observed from the *later stage* in Fig. 3(a) that eventually a huge unbalanced behavior appears and the capacities of the exits are not efficiently utilized. The typical example of pedestrian distribution at the “stage 3” is shown in Fig. 4(d) with the time instant given by  $k = 60$ . It can be found from the figure that most of the remaining pedestrians are attracted by the exits 3 and 4 but not all the exits.

Recalling that the unbalanced pedestrian densities may bring a larger travel time  $T_{\text{end}}$  since the capacities of the exits are not efficiently utilized, we begin to present the simulation results with different density control strategies which adjust the guiding strength of the evacuation assistants and hence affect the pedestrian densities near the exits in the following sections.

### 3.3. Simulation Results with Bang-bang Control

#### 3.3.1. An Example Showing Controllable Pedestrian Density

In this section, we present the simulation results with Bang-bang control where the guiding coefficients  $u_i(k)$ ,  $k = 1, 2, \dots, \infty$ , are updated by Eq. (6) for each  $i \in \mathcal{N}$  with the target density to be  $\rho_{\text{aim}} = 0.5$ . In this case, each of the evacuation assistants shuts down the guiding signal if the actual pedestrian density is in excess of  $\rho_{\text{aim}}$  but turns it on for the reverse situation. In the simulation, it is found that the pedestrians used 96 time steps to leave the state space, i.e.,  $T_{\text{end}} = 96$ , which is slightly shortened comparing to the non-control scenario. The trajectories of the pedestrian densities near the four exits and the corresponding unbalanced degrees  $\alpha_i(k)$ ,  $i \in \mathcal{N}$ , are shown in Fig. 3(b). The pedestrian distributions at time instants  $k = 10, 30, 40$  and  $60$  are illustrated in Fig. 5 (same instants as Fig. 4). It can be seen from those figures that the herding effects generated from mutual attractions among pedestrians in stage 2 are obviously suppressed under the density control (see Figs. 5(b) and 5(c)) and hence the pedestrian densities around the four exits possess a low unbalanced degree for a longer period in Fig. 3(b). Moreover, since the pedestrian distribution is more balanced, the period of stage 3 with a huge unbalanced density degree is certainly shortened.

It is worth to note that the above simulation results provide an interesting insight in that the unbalanced density degree is controllable by adjusting the guiding strength of the evacuation assistants according to the real-time data of pedestrian densities, which may eventually shorten the travel time and hence improve the efficiency of the evacuation process. To check whether there exists and why there exists an optimized target density, we characterize the influence of the target density  $\rho_{\text{aim}}$  on pedestrian behaviors under the density control law in Eq. (6) in the next section.

#### 3.3.2. Influence of the target density in Bang-bang control

In this section, we note that not all of the density control behaviors could improve evacuation efficiency but a certain set of the target pedestrian density. The response of target density on travel time of evacuation is shown in Fig. 6 below. It is interesting to see that the travel time  $T_{\text{end}}$  is shortened under the Bang-bang density control law Eq. (6) when the target density is moderate (around  $0.22 < \rho_{\text{aim}} < 0.6$ ), and is enlarged when the target is too small ( $\rho_{\text{aim}} < 0.22$ ). We note that the response curve characterized in Fig. 6 is very nature in the sense of physical meaning. If the target density  $\rho_{\text{aim}}$  is very large for the Bang-bang density control law in Eq. (6), then the pedestrian behaviors are very similar to the ones without density control since it follows from Eq. (6) that the guiding signals

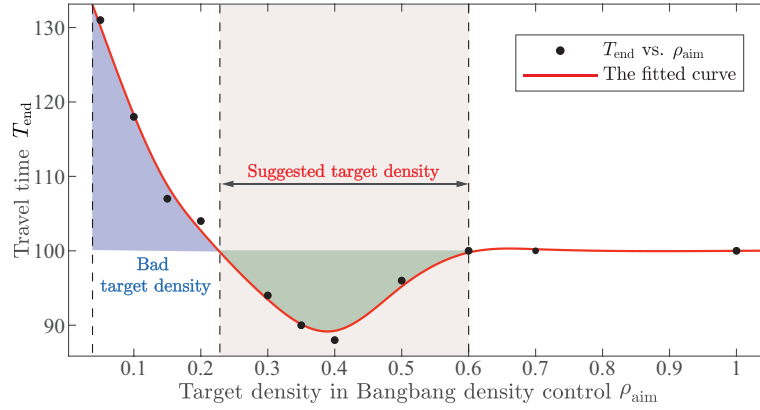


Figure 6. Response of the target density on travel time under Bang-bang control.

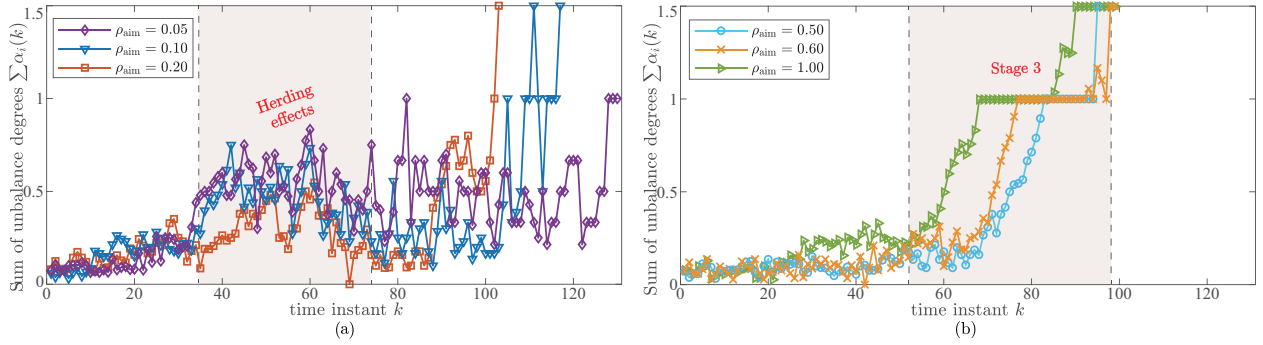


Figure 7. The influence of the target density on the summation of the unbalanced degrees under Bang-bang control. The herding effects and the stage 3 are suppressed and prolonged in (a) and (b) respectively when the target density increases.

are almost turned on for all the time instants. Reversely, if the target is very small, then the herding effects among the pedestrians would lead extremely unbalanced distribution during the evacuation process and hence enlarge the travel time, because the guiding signals are shut down at most of the time instants. In this case, the pedestrians are not guided by any evacuation assistant and only move according to the mutual attractions among themselves.

To be precise, we verify the above analysis by studying the influence of target density on the unbalanced degrees during the evacuation process. The trajectories of the summation of the unbalanced degrees with the target densities given by  $\rho_{\text{aim}} \in \{0.05, 0.1, 0.2\}$  and  $\rho_{\text{aim}} \in \{0.5, 0.6, 1.0\}$  are illustrated in Figs. 7(a) and 7(b), respectively. It can be seen from Fig. 7(a) that when the target density is very small, the herding effects among pedestrians which lead to unbalanced distributions in stage 2 are extremely huge, but can be suppressed by increasing the target density. However, Fig. 7(b) indicates that the Bang-bang control with a too large target density cannot suppress the herding effects well any more and the pedestrian distributions become more unbalanced when the target density increases. As the typical examples, Fig. 8(a) shows that the evacuation assistant needs a long time to achieve the control task for a too small target density (e.g.,  $\rho_{\text{aim}} = 0.2$ ), and Fig. 8(b) shows that the pedestrian density is initially under control but lost of control soon for a too large target density (e.g.,  $\rho_{\text{aim}} = 0.6$ ). Consequently, our results demonstrate that to guarantee the well controlled pedestrian density for the entire evacuation process (i.e., to achieve the density control soon and avoid a losing of control), it is required to pick a target density as a middle value (e.g., among 0.2 and 0.6).

### 3.3.3. Shortness of Bang-bang Control: Sacrificing the efficiency during the early stage

On the one hand, although the Bang-bang density control scheme in Eq. (6) with a properly designed target density indeed improves the evacuation efficiency, it is surprised to observe that the pedestrians remaining in the state space under Bang-bang control are more than the case without density control for each of the time instants shown in Figs. 4 and 5. Hence, we conclude that the density balance contributing to shorten the total travel time by Bang-bang control is yielded from sacrificing the efficiency during the early stage of the evacuation process (see the solid proof from simulation in Section 3.4 below). Recalling that the fundamental factor affecting the evacuation efficiency is the efficient and balanced utilization of all the exits, the Bang-bang control scheme in Eq. (6) maybe not a best choice for



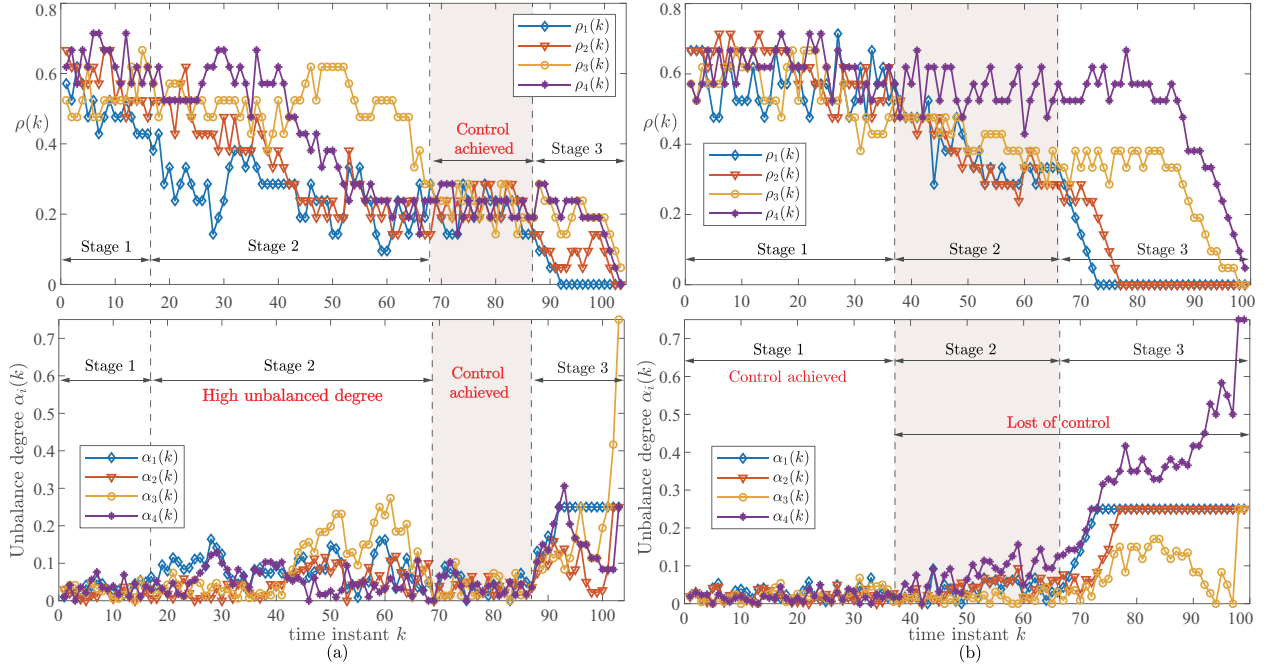


Figure 8. Trajectories of pedestrian densities and unbalanced degrees under Bang-bang control with *bad* target density  $\rho_{\text{aim}}$ . (a):  $\rho_{\text{aim}} = 0.2$ , (b):  $\rho_{\text{aim}} = 0.6$ . In (a), the control task is achieved after a while. In (b), the pedestrian densities are initially controlled well but lost of control soon.

the guiding strength update laws to improve the evacuation efficiency. It is natural to ask that is there any other control scheme to guarantee not only the balanced pedestrian densities but also the efficient utilization of the exits. On the other hand, we note that the Bang-bang control is pretty *sensitive* with respect to the observed (current) density value, which may be the reason of efficiency loss in the evacuation process. Hence, we present the results simulated by a different control scheme in the following section.

### 3.4. Simulation Results with PI Control

In this section, we present the simulation results under the PI control scheme with  $K_p = 70$  and  $K_i = 20$ , where the guiding coefficients  $u_i(k)$ ,  $k = 1, 2, \dots, \infty$ , are updated by Eq. (7) for each  $i \in \mathcal{N}$ . In this case, instead of using an on-off guiding signal, each of the evacuation assistants may slightly adjust the guiding coefficient from 0 to 1 when there is a density error between the real-time density and the target density.

The response of target density on travel time of evacuation is shown in Fig. 9. It can be seen from the figure that the tendency of the response curve generated by PI control is very similar to the one by Bang-bang control, but the

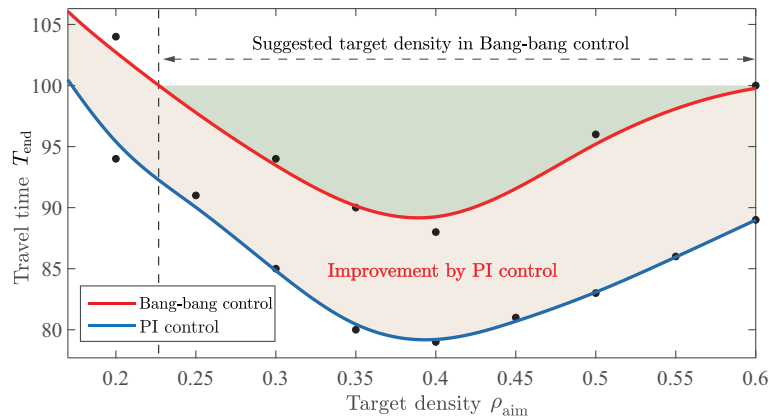


Figure 9. Comparison of travel time response with respect to target densities for PI control in Eq. (7) and Bang-bang control in Eq. (6). The evacuation efficiency is improved by PI control for the suggested target density of the Bang-bang control.

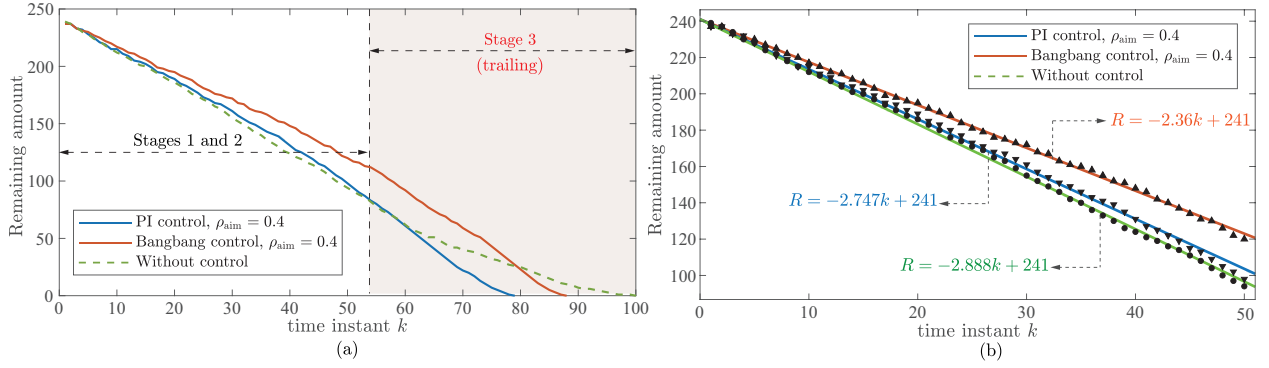


Figure 10. Amount of remaining pedestrians in the state space under cases of non-control, Bang-bang control and PI control with the optimized target density. Note that (b) is the copy of (a) with fitted straight lines, which shows that in the first 50 time instants, around 2.888, 2.747 and 2.36 pedestrians left the state space per each time instant.

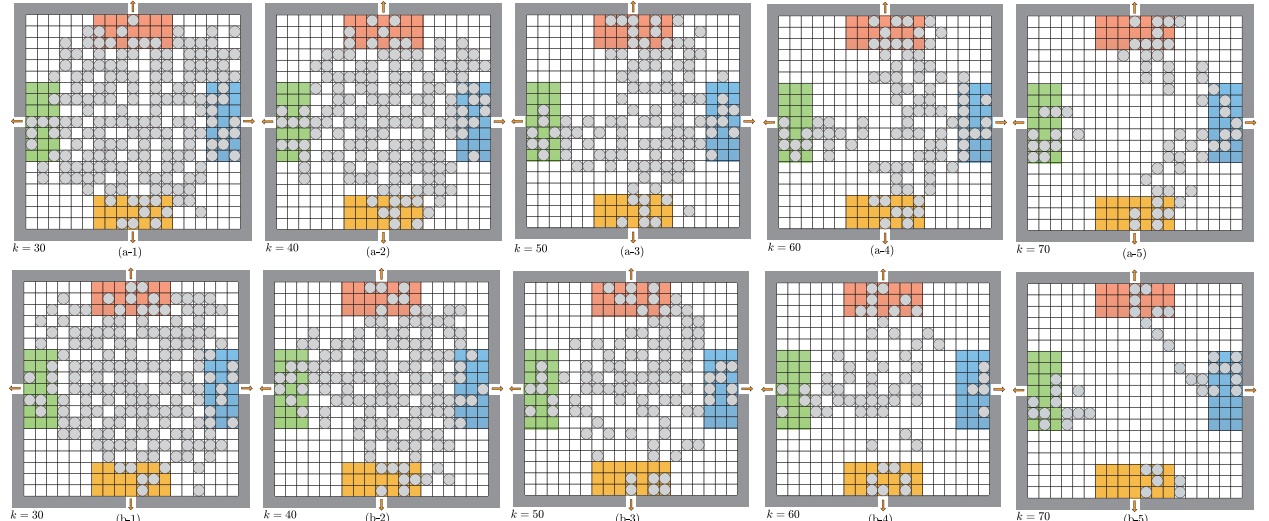


Figure 11. Pedestrian distributions at the typical time instants under Bang-bang and PI control with  $\rho_{aim} = 0.4$ . (a): Bang-bang, (b): PI. The crowd in the middle in (a) keeps moving to the right side and the tendency is not suppressed by the Bang-bang control in (a-3)–(a-5). But the tendency is keeping corrected to the reverse directions by the PI control in (b-3)–(b-5). That is to say, the density control for the *partial regions* (near the exits) could yield a better *global effect* for balancing the pedestrians in the *rest of the regions* if we use the PI control than Bang-bang control.

evacuation efficiency is significantly improved. The reason why a too large or too small target density brings a bigger travel time is already interpreted in Section 3.3.2, that is, a too large target density leads to a *loss of control* soon and a too small target density leads a *long time* for achieving the control task.

Now, we study the principle of why PI control improves the evacuation efficiency by making comparisons with the cases of non-control and Bang-bang control. The amounts of remaining pedestrians simulated for the PI control and Bang-bang control under the best target density  $\rho_{aim} = 0.4$  are shown in Fig. 10 along with the trajectory for the non-control case. All of the trajectories possesses an almost liner tendency in the early stage of the evacuation process. But the trajectory for the non-control case possesses an obvious “tail” (caused by the unbalanced pedestrian distribution) in the later stage (which is referred to as stage 3 in Section 3.2) during which the evacuation efficiency declines significantly. Note that the corresponding trajectories of the density at stage 3 are already given in Fig. 4(a) above. After we apply the Bang-bang control, the “obvious tail” is indeed eliminated and hence the total travel time is shortened. Moreover, Fig. 10(a) further verifies our analysis given in Section 3.3.3 in the sense that the illustrated curves for Bang-bang control is much gentler than the one without control. In particular, it follows from the fitted lines of the first 50 time instants shown in Fig. 4(b) that around 2.888 pedestrians left the state space per each time instant for the non-control case, but only 2.36 pedestrians left under Bang-bang control, which indicates that the elimination of the “obvious tail” via Bang-bang control is made by sacrificing the efficiency during the *early stage*.

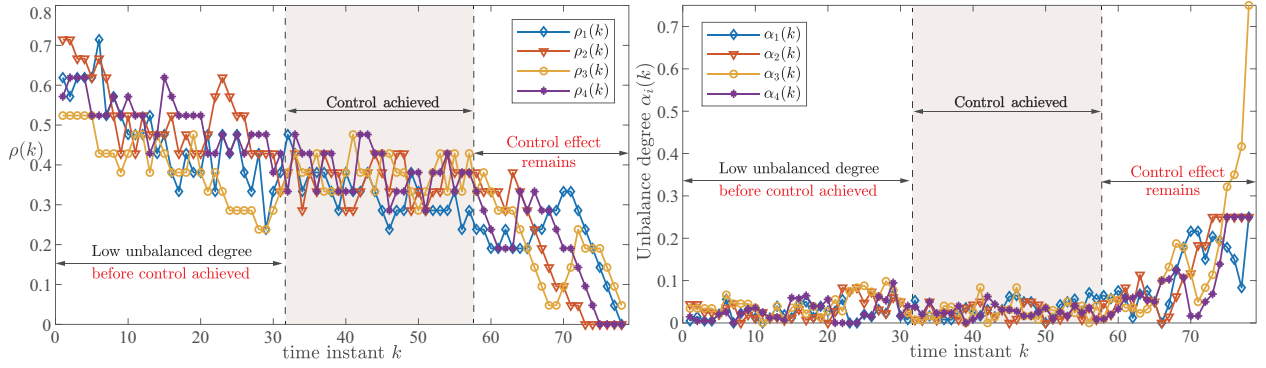


Figure 12. Trajectories of pedestrian densities and unbalanced degrees under designed density control scheme (PI control with  $\rho_{\text{aim}} = 0.4$ ). The control target is well achieved comparing to the curves shown in Figs. 4 and 8.

However, for the PI control case, it can be seen from Fig. 10(a) that the “obvious tail” is eliminated without losing too much efficiency. Besides, the pedestrian distributions shown in Fig. 11 demonstrate that the PI control possesses a better global performance for balancing the pedestrian distribution in the entire state space than the Bang-bang control, because the crowd in Fig. 11(a) keeps moving towards the right-hand side in an unbalanced way without any obvious suppressions, but the unbalanced tendency in Fig. 11(b) keeps being corrected to the reverse directions (see Fig. 11(b-3)–(b-5)). For the convenience of the reader to make a comparison with the trajectories shown in Figs. 3 and 8, we illustrate the trajectories of pedestrian densities and unbalanced degrees under PI control with the optimized target density in Fig. 12, which shows an almost synchronization behavior during the entire evacuation process. The above results give an important insight into designing the guiding strategies in the real evacuation process.

#### 4. Conclusion

To reveal the possibility of enhancing guided evacuation efficiency by imposing control schemes, in this paper, we investigated the effect of variable guiding strategies in a multi-exits evacuation process. Specifically, we proposed a force-driven cellular automaton model with adjustable guiding attractions imposed by the evacuation assistants located in the exits. In this model, each of the evacuation assistants tries to attract the pedestrians towards its own exit by sending a quantifiable guiding signal, which may be adjusted according to the values of pedestrian density near the exit. In accordance to the cases with and without density control, the simulation results were respectively established.

According to the evidence shown in the simulation, we first revealed the fact that an inherent problem of *unbalanced* pedestrian distribution exists in the multi-exits evacuation process, i.e., an extremely unbalanced pedestrian distribution exists in the later stage of the evacuation process, which eventually leads to inefficient utilization of the exits. Our results showed that the *unbalanced* pedestrian distribution is mainly yielded by a snowballing effect generated from the mutual attractions among the pedestrians, and can be suppressed by partially controlling the pedestrian densities around the exits. We considered the effects of the density controls in an on-off fashion (i.e., Bang-bang control) and a quantifiable fashion (i.e., PI control) to adjust the guiding strength for each of the evacuation assistants. A moderate value representing the optimized target density for both of the Bang-bang control and PI control was found. It was revealed that the efficiency improvement of Bang-bang control is based on sacrificing the efficiency during the early stage, but the one for PI control is yielded without losing too much efficiency during the early stage and hence PI control further improves the evacuation efficiency. Since we showed that the density control for the partial regions (near the exits) could yield a global effect for balancing the pedestrians in the rest of the regions, our results are expected to give some interesting and important insights to design the guiding strategies in the real evacuation process.

However, the control performance of Bang-bang control and PI control might be strongly connected to the morphic conditions of the evacuation space including the number of exits [34], asymmetric degree of exits [35] and sampling regions. For yielding more general result, the analysis on those factors may be promised necessary future research directions. The other future directions may include the extensions to multi-exits coordination and the game formulations between different clusters [36].

## Acknowledgments

This work was supported jointly by Program for Young Excellent Talents in University of Fujian Province (201847) and China Scholarship Council (201908050058).

## References

- [1] Q. Meng, M. Zhou, J. Liu, H. Dong, Pedestrian evacuation with herding behavior in the view-limited condition, *IEEE Trans. Comput. Soc. Syst.* 6 (3) (2019) 567–575. doi:<https://doi.org/10.1109/TCSS.2019.2915772>.
- [2] Y. Cheng, X. Zheng, Emergence of cooperation during an emergency evacuation, *Appl. Math. Comput.* 320 (2018) 485–494. doi:<https://doi.org/10.1016/j.amc.2017.10.011>.
- [3] M. Haghighi, E. Cristiani, N. W. Bode, M. Boltes, A. Corbetta, Panic, irrationality, and herding: three ambiguous terms in crowd dynamics research, *J. Adv. Transp.* 2019. doi:<https://doi.org/10.1155/2019/9267643>.
- [4] J. Guan, K. Wang, Towards pedestrian room evacuation with a spatial game, *Appl. Math. Comput.* 347 (2019) 492–501. doi:<https://doi.org/10.1016/j.amc.2018.11.003>.
- [5] G. G. Løvås, Modeling and simulation of pedestrian traffic flow, *Transp. Res. Part B* 28 (6) (1994) 429–443. doi:[https://doi.org/10.1016/0191-2615\(94\)90013-2](https://doi.org/10.1016/0191-2615(94)90013-2).
- [6] D. Helbing, I. Farkas, T. Vicsek, Simulating dynamical features of escape panic, *Nature* 407 (6803) (2000) 487–490. doi:<https://doi.org/10.1038/35035023>.
- [7] F. Müller, O. Wohak, A. Schadschneider, Study of influence of groups on evacuation dynamics using a cellular automaton model, *Transp. Res. Rec.* 2 (2014) 168–176. doi:<https://doi.org/10.1016/j.trpro.2014.09.022>.
- [8] D. Yanagisawa, K. Nishinari, Mean-field theory for pedestrian outflow through an exit, *Phys. Rev. E* 76 (2007) 061117. doi:<https://doi.org/10.1103/PhysRevE.76.061117>.
- [9] A. Varas, M. Cornejo, D. Mainemer, B. Toledo, J. Rogan, V. Munoz, J. Valdivia, Cellular automaton model for evacuation process with obstacles, *Physica A* 382 (2) (2007) 631–642. doi:<https://doi.org/10.1016/j.physa.2007.04.006>.
- [10] K. Huang, X. Zheng, Y. Cheng, Y. Yang, Behavior-based cellular automaton model for pedestrian dynamics, *Appl. Math. Comput.* 292 (2017) 417–424. doi:<https://doi.org/10.1016/j.amc.2016.07.002>.
- [11] R. Alizadeh, A dynamic cellular automaton model for evacuation process with obstacles, *Saf. Sci.* 49 (2) (2011) 315–323. doi:<https://doi.org/10.1016/j.ssci.2010.09.006>.
- [12] S. Cao, L. Fu, W. Song, Exit selection and pedestrian movement in a room with two exits under fire emergency, *Appl. Math. Comput.* 332 (2018) 136–147. doi:<https://doi.org/10.1016/j.amc.2018.03.048>.
- [13] Z. Shahhoseini, M. Sarvi, Pedestrian crowd flows in shared spaces: investigating the impact of geometry based on micro and macro scale measures, *Transp. Res. Part B* 122 (2019) 57–87. doi:<https://doi.org/10.1016/j.trb.2019.01.019>.
- [14] K. Huang, X. Zheng, Y. Yang, T. Wang, Behavioral evolution in evacuation crowd based on heterogeneous rationality of small groups, *Appl. Math. Comput.* 266 (2015) 501–506. doi:<https://doi.org/10.1016/j.amc.2015.05.065>.
- [15] M. Chraïbi, A. Seyfried, A. Schadschneider, Generalized centrifugal-force model for pedestrian dynamics, *Phys. Rev. E* 82 (4) (2010) 046111. doi:<https://doi.org/10.1103/PhysRevE.82.046111>.
- [16] W. Liao, X. Zheng, L. Cheng, Y. Zhao, Y. Cheng, Y. Wang, Layout effects of multi-exit ticket-inspectors on pedestrian evacuation, *Saf. Sci.* 70 (2014) 1–8. doi:<https://doi.org/10.1016/j.ssci.2014.04.015>.
- [17] Y. Hao, Z. Bin-Ya, S. Chun-Fu, X. Yan, Exit selection strategy in pedestrian evacuation simulation with multi-exits, *Chin. Phys. B* 23 (5) (2014) 050512. doi:<https://doi.org/10.1088/1674-1056/23/5/050512>.
- [18] P. Hrabak, M. Bukacek, Influence of agents heterogeneity in cellular model of evacuation, *J. Comput. Sci.* 21 (2017) 486–493. doi:<https://doi.org/10.1016/j.jocs.2016.08.002>.
- [19] C. K. Chen, J. Li, D. Zhang, Study on evacuation behaviors at a T-shaped intersection by a force-driving cellular automata model, *Physica A* 391 (7) (2012) 2408–2420. doi:<https://doi.org/10.1016/j.physa.2011.12.001>.
- [20] X. Li, F. Guo, H. Kuang, Z. Geng, Y. Fan, An extended cost potential field cellular automaton model for pedestrian evacuation considering the restriction of visual field, *Physica A* 515 (2019) 47–56. doi:<https://doi.org/10.1016/j.physa.2018.09.145>.
- [21] K. Huang, X. Zheng, A weighted evolving network model for pedestrian evacuation, *Appl. Math. Comput.* 298 (2017) 57–64. doi:<https://doi.org/10.1016/j.amc.2016.10.040>.
- [22] L. A. Pereira, D. Burgarelli, L. Duczmal, F. Cruz, Emergency evacuation models based on cellular automata with route changes and group fields, *Physica A* 473 (2017) 97–110. doi:<https://doi.org/10.1016/j.physa.2017.01.048>.
- [23] D. Miyagawa, G. Ichinose, Cellular automaton model with turning behavior in crowd evacuation, *Physica A: Statistical Mechanics and its Applications* (2020) 124376 doi:<https://doi.org/10.1016/j.physa.2020.124376>.
- [24] X. Yang, H. Dong, X. Yao, X. Sun, Q. Wang, M. Zhou, Necessity of guides in pedestrian emergency evacuation, *Physica A* 442 (2016) 397–408. doi:<https://doi.org/10.1016/j.physa.2015.08.020>.
- [25] Y. Ma, R. K. K. Yuen, E. W. M. Lee, Effective leadership for crowd evacuation, *Physica A* 450 (2016) 333–341. doi:<https://doi.org/10.1016/j.physa.2015.12.103>.
- [26] Y. Ma, E. W. M. Lee, M. Shi, Dual effects of guide-based guidance on pedestrian evacuation, *Mod. Phys. Lett.* 381 (22) (2017) 1837–1844. doi:<https://doi.org/10.1016/j.physleta.2017.03.050>.
- [27] M. Zhou, H. Dong, P. A. Ioannou, Y. Zhao, F.-Y. Wang, Guided crowd evacuation: approaches and challenges, *IEEE/CAA Journal of Automatica Sinica* 6 (5) (2019) 1081–1094. doi:<https://doi.org/10.1109/JAS.2019.1911672>.
- [28] M. Zhou, H. Dong, Y. Zhao, P. A. Ioannou, F.-Y. Wang, Optimization of crowd evacuation with leaders in urban rail transit stations, *IEEE Trans. Intell. Transp. Syst.* 20 (12) (2019) 4476–4487. doi:<https://doi.org/10.1109/TITS.2018.2886415>.

- [29] S. Long, D. Zhang, S. Li, S. Yang, B. Zhang, Simulation-based model of emergency evacuation guidance in the metro stations of China, IEEE Access 8 (2020) 62670–62688. doi:<https://doi.org/10.1109/ACCESS.2020.2983441>.
- [30] X. Yang, X. Yang, Q. Wang, Y. Kang, F. Pan, Guide optimization in pedestrian emergency evacuation, Appl. Math. Comput. 365 (2020) 124711. doi:<https://doi.org/10.1016/j.amc.2019.124711>.
- [31] H. Kurdi, A. Almulifi, S. Al-Megren, K. Youcef-Toumi, A balanced evacuation algorithm for facilities with multiple exits, Eur. J. Oper. Res. 289 (2021) 285–296. doi:<https://doi.org/10.1016/j.ejor.2020.07.012>.
- [32] J. Tanimoto, A. Hagishima, Y. Tanaka, Study of bottleneck effect at an emergency evacuation exit using cellular automata model, mean field approximation analysis, and game theory, Physica A 389 (24) (2010) 5611–5618. doi:<https://doi.org/10.1016/j.physa.2010.08.032>.
- [33] J. Tanimoto, Evolutionary games with sociophysics: Analysis of traffic flow and epidemics, Springer, 2019. doi:<https://doi.org/10.1007/978-981-13-2769-8>.
- [34] H. A. Kurdi, S. Al-Megren, R. Althunyan, A. Almulifi, Effect of exit placement on evacuation plans, Eur. J. Oper. Res. 269 (2) (2018) 749–759. doi:<https://doi.org/10.1016/j.ejor.2018.01.050>.
- [35] H. Yue, H. Guan, C. Shao, X. Zhang, Simulation of pedestrian evacuation with asymmetrical exits layout, Physica A 390 (2) (2011) 198–207. doi:<https://doi.org/10.1016/j.physa.2010.10.003>.
- [36] J. Tanimoto, Fundamentals of evolutionary game theory and its applications, Springer, 2015. doi:<https://doi.org/10.1007/978-4-431-54962-8>.